Technical Sciences, 2020, 23(1), 25–51

UNIWERSYTET WARMIŃSKO-MAZURSKI W OLSZTYNIE

Quarterly peer-reviewed scientific journal
ISSN 1505-4675
e-ISSN 2083-4527
TECHNICAL SCIENCES
Homepage: www.uwm.edu.pl/techsci/

doi: 10.31648/ts.4863

TIME CONSUMPTION IN CALCULATIONS OF HYDRAULIC AND GEOMETRICAL TORTUOSITY IN GRANULAR BEDS

Wojciech Sobieski[1], Amir Raoof[2], Alraune Zech[3]

[1]ORCID: 0000-0003-1434-5520
Department of Mechanical Engineering and Fundamentals of Machine Design
University of Warmia and Mazury in Olsztyn, Poland
[2]ORCID: 0000-0003-1613-6546
Environmental Hydrogeology, Department of Earth Sciences
Utrecht University, Netherlands
[3]ORCID: 0000-0002-8783-6198
Environmental Hydrogeology, Department of Earth Sciences
Utrecht University, Netherlands

Received 20 December 2019, accepted 6 April 2020, available online 27 April 2020.

Keywords: granular porous media, geometric tortuosity, hydraulic tortuosity, Path Tracking Method, Discrete Element Method, Lattice Boltzmann Method.

Abstract

Tortuosity is one of the most elusive porous media parameters due to its subjective estimation. Here, we compare two approaches for obtaining tortuosity in granular porous media to investigate their capabilities and limitations. First, we determine the hydraulic tortuosity based on the calculated components of the velocity field obtained from flow simulations using the Lattice Boltzmann Method (LBM). Second, we directly determine the geometric tortuosity by making use of the Path Tracking Method (PTM) which only requires the geometric properties of the porous medium. In both cases, we apply the same geometrical structure which is a virtually generated 3D granular bed using the Discrete Element Method consisting of 50 particles. Our results show that the direct PTM is much faster and more precise than the indirect approach based on the calculated velocity field. Therefore, PTM may provide a tool for calculating tortuosity for large 3D granular systems where indirect methods are limited due to the required computational power and time. While LBM considers

Correspondence: Wojciech Sobieski, Katedra Mechaniki i Podstaw Konstrukcji Maszyn, Wydział Nauk Technicznych, Uniwersytet Warmińsko-Mazurski, ul. M. Oczapowskiego 11, 10-957 Olsztyn, phone +48 (89) 523 32 40, e-mail: wojciech.sobieski@uwm.edu.pl.

various routes across the porous media implicitly, PTM identifies them explicitly. As a result, PTM requires a statistical post-processing. As an advantage, this can provide further information than just domain scale average values.

Introduction

Granular porous media is ubiquitous in nature and is applied widely in industry, as fuel cells and chemical reactors. Thus, predicting its physical properties is highly desirable. Of particular interest are systems with a solid phase and one or more fluid phases occupying the pore space.

The growing interest in multiphase systems triggered the development of hybrid numerical methods. Table 1 provides a selected overview of such methods in the context of porous media. Conceptually, hybrid methods couple a numerical code to track the solid phase with a solver for fluid movement within the pore space. Different components are either weakly or strongly coupled; meaning that:

– data is passed only from one method to the other once, no back transfer;

– data is transferred back and forth between both components, usually in an external calculation loop (e.g. within one time step).

The strong coupling usually requires significant adaptions to both numerical codes. Hybrid models often feature Open Source software (*Free Software Foundation* 2020).

The application of hybrid models is computationally demanding. Simulation times of days, weeks or even months are not unusual which limits their applications, particularly in the context of non-deterministic granular media. The problem amplifies when data transfer or geometry conversion is needed.

Hybrid methods are used to investigate the geometrical structure of granular porous media. In such a case, one method serves to generate the geometry of the porous body; usually a random algorithm or a Discrete Element Method (DEM) is applied. The second method is used to characterize features and parameters of the pore space; often Finite Volume Method (FVM) or Lattice Boltzmann Method (LBM) are in use.

Of particular interest for us is the tortuosity, which characterizes the prolongation of flow paths due to the granular porous structure. It is often associated to how intertwined paths through the granular media are. This geometrical parameter is a significant characteristic of granular medium, but at the same time difficult to obtain.

Tortuosity (τ[-]) is defined as the ratio of an average path length (L_p [m]) in the void space of a porous medium to the thickness of the porous body (L_0 [m]) (Bear 1972):

$$\tau = \frac{L_p}{L_0} \tag{1}$$

Table 1

Hybrid models used for granular porous media and to simulate fluid flow

Source	Methods (software)	Application
FENG et al. (2007)	DEM & LBM	particle transport in turbulent fluid flows
ROJEK (2007)	DEM & FEM (Simpact)	rock cutting
CHEN (2009)	DEM (YADE, PFC2D) & FVM (OpenFoam)	fluid flow through an assembly of particles
SOBIESKI (2009)	DEM (PFC3D, YADE) & PTM	geometrical structure of granular beds
VILLARD et al. (2009)	FEM & DEM	earth structures reinforced by geosynthetic
ERATH (2010)	FEM & BEM	numerical analysis of coupling
DUDA et al. (2011)	LBM	fluid flow through a porous medium (with self-generated geometry)
WU et al. (2011)	FEM & FVM-VOF	moving obstacle in fluid
CATALANO (2012)	DEM (YADE) & PFV (own model)	biphasic granular media
KOMORÓCZI et al. (2012)	DEM & SPH	boudinage, hydro-fracturing
STRÁNSKÝ, JIRÁSEK (2012)	FEM (OOFEM) & DEM (YADE)	cantilever shock analysis
XIANG et al. (2012)	FEM & DEM; (FEMDEM)	breakwater modelling
GALINDO-TORRES (2013)	DEM & LBM	fluid-solid interaction with particles of general shapes
SRIVASTAVA et al. (2013)	FEM & DEM	fluid-particle interactions
SUN et al. (2013)	DEM (OVAL) &-LBM	permeability evolutions inside a dilatants shear band
ZHAO, SHAN (2013)	FVM (OpenFOAM) & DEM (LAMMPS, LIGGGHTS)	fluid-particle interaction
MAREK (2014)	DEM & IBM	fluid flow through an assembly of Raschig rings (with self-generated geometry)
NORDBOTTEN (2014)	FEM (Visage) & FVM (Eclipse)	Hydro-mechanical simulation in porous media
AFKHAMI et al. (2015)	LES (Fluent) & DEM (EDEM)	particle interaction and agglomeration in a turbulent channel flow
MARKL (2015)	LBM (waLBerla) & DEM (pe)	beam melting
QIU (2015)	DEM & LBM	fluid flow through porous media
ZENG, YAO (2015)	DFM & FEM	fractured porous media
MAHABADI et al. (2016)	FEM-DEM; (Irazu)	rocks mechanics
MARKAUSKAS et al. (2016)	DEM & SPH and DEM & FVM (Fluent)	particle-fluid Poiseuille flow in a channel

cont. Table 1

SAKAI (2016)	SPH & MPS	fluidisation, circulating flow, screw conveyor, twin-screw kneader
TRYKOZKO et al. (2016)	FVM	fluid flow through a porous medium (with self-generated geometry)
AL-ARKAWAZI et al. (2017)	DEM (SIGRAME) & FVM (Code_Saturne)	fluidisation

DEM – Discrete Element Method, FVM – Finite Volume Method, IBM – Immersed Boundary Method, PFV – Pore-scale Finite Volume, LES – Large Eddy Simulation, FEM – Finite Element Method, LBM – Lattice Boltzmann Method, BEM – Boundary Element Method, SPH – Smoothed Particle Hydrodynamics, DFM – Discrete Fractured Model, PTM – Path Tracking Method.

The definition holds for tortuosity calculations in 2D or 3D space. Note that L_p is at minimum the length of L_0. Thus, physically reasonable values of τ are always higher or equal one. The above definition requires the existence of free passages through the porous body. We limit our investigation to granular media where pore space forms a connected network through which fluid flow is possible independent of the domain size and the particle distribution.

In general, the tortuosity of a specific granular medium is either calculated based on the pore channels geometry (geometrical tortuosity, τ^g) or based on the ratios of velocity components in a creeping fluid flow (hydraulic tortuosity, τ^h). Other kinds of tortuosity are also known, e.g. diffusional (GHAREDAGHLOO et al. 2018) or electric tortuosity (SAOMOTO, KATAGIRI 2015). In some works, the Minkowski space is applied to analyse the tortuosity of porous media (CIESZKO, KRIESE 2006, CIESZKO 2009). The geometrical tortuosity can be determined by direct calculations, following the definition in Equation 1. One of these methods is the Path Tracking Method (SOBIESKI 2009, SOBIESKI et al. 2012). Hydraulic tortuosity requires the application of hybrid methods (Tab. 1), combining geometry generation and flow simulations. Besides standard techniques as Finite Difference, Finite Element or Finite Volume Methods, the Lattice Boltzmann Method is particularly attractive in the context of porous media due to its simple geometry specification. Geometries as well as velocity fields may as well be determined by experimental techniques, such as Particle Image Velocimetry (PIV) (WILLERT, GHARIB 1991).

KOPONEN et al. (1996, 1997) proposed to calculate the hydraulic tortuosity as

$$\tau^h = \frac{\sum v}{\sum v_x} \tag{2}$$

where:

v_x – the velocity component in the direction of macroscopic flow in the porous material [m/s],

v – the absolute velocity magnitude [m/s].

The sums go over the entire pore space. The specification of τ^h (Eq. 2) follows the conceptualization of tortuosity in a capillary tube model by CARMAN (1937). However, τ^h as in Equation 2 has no direction connection with the actual flow path and is determined solely through fluctuations of the local flow field around the average flux in main flow direction.

KOPONEN et al. (1996) investigated the lattice gas flow through 2D random porous media where the macroscopic parameters of the fluid are simple functions of the lattice gas distribution function. The work of KOPONEN et al. (1997) and following work based on the same methodology (DUDA et al., 2011, NABOVATI, SOUSA 2007) are limited to flow in 2D random porous media with rectangular solid particles. There are less studies applying the methodology in 3D due to the tremendous computational effort to calculate the velocity field in 3D (WANG 2014).

In this study, we compare two conceptually different methodologies for obtaining tortuosity in 3D granular beds. We determine hydraulic tortuosity following the idea of KOPONEN et al. (1996, 1997) and we calculate the geometric tortuosity making use of the Path Tracking Method. To compare the two methods, we apply them using the same virtually created granular structure.

Materials and Methods

Granular Material

Starting point for the method comparison is a virtual realization of a granular structure. We create one bed consisting of 50 spherical particles placed in a cuboid domain. Particle sizes are based on marble glass beads used in previous experimental investigations (SOBIESKI et al. 2016b) SiLibeads Glass Type S (LINDNER 2015). These grains have an average diameter equal to 6.072 mm and a standard deviation of 0.051.

Discrete Element Method

We created the virtual granular bed using the Discrete Element Method (DEM) proposed by CUNDALL and STRACK (1979). DEM evaluates the dynamics of a set of solid bodies using Newtonian laws of linear and angular motion:

$$m_i \frac{\mathrm{d}\vec{v}_i}{\mathrm{d}t} = \sum_{j=1}^{n_c} \left(\vec{F}_{ij}^{\,n} + \vec{F}_{ij}^{\,t}\right) + \vec{F}_i^{\,\mathrm{ext}} \tag{3}$$

and

$$I_i \frac{\mathrm{d}\vec{\omega}_i}{\mathrm{d}t} = \sum_{j=1}^{n_c} \left(r_i \times \vec{F}_{ij}^{\,t} + f_{ij} \times \vec{F}_{ij}^{\,n}\right) \tag{4}$$

where:

m_i – mass of the i-th body [kg],
I_i – moment of inertia of the i-th body [kg·m^2],
$\vec{v}_i$ – linear velocity of the i-th body [m/s],
$\vec{\omega}_i$ – angular velocity of the i-th body [rad/s],
$\vec{F}_{ij}^{n}$ – normal forces between neighbouring bodies i and j [N],
$\vec{F}_{ij}^{t}$ – tangential forces between neighbouring bodies i and j [N],
n_c – number of contacts between i-th body and neighbouring bodies [-],
$\vec{F}_i^{\text{ext}}$ – external forces acting on the i-th body (e.g. gravity force) [N],
r_i – distance between the contact point with the j-th body and the mass centre of the i-th body [m],
f_{ij} – distance between the direction of acting the normal force and the mass centre [m].

The algorithm consists of three main steps:

– detecting all contact pairs;

– calculating new values of forces acting on each body (velocities and displacements are constant in this stage);

– calculating new values of velocities and displacements (forces are constant in this stage).

The key aspect is the mathematical description of the normal and tangential forces between bodies in all contact points. Thus, their calculation in every time step is particularly important.

The physically based DEM approach is advantageous to simple random generators for constructing 3D porous structures since it takes particle interactions into account. That allows to create virtual beds with smaller porosity.

We created the specific virtual granular bed using the Radius Expansion Method (WIDULIŃSKI et al. 2009), implemented in the open source code YADE (ŠMILAUER et al. 2017). The final geometry is fully characterized by the centre coordinates of particles (x_m, y_m, z_m) (m = 1, …, 50) and their radii r_m (or diameter d_m). From that, geometrical characteristics such as porosity can calculated.

Lattice Boltzmann Method

The Lattice Boltzmann Method (LBM) is used to calculate the flow on the porous grain structure. The flow of a fluid is characterized by the discrete Boltzmann equation (BHATNAGAR et al. 1954):

$$\frac{\partial f}{\partial t} + \vec{v}\nabla_{\vec{x}} f + \frac{\vec{F}}{m}\nabla_{\vec{v}} f = \left(\frac{\partial f}{\partial t}\right)_{\text{col}} \tag{5}$$

where:

$f(x, v, t)$ – single-particle distribution function (where x is the coordinate and v is the microscopic velocity),

$\frac{\vec{F}}{m}$ – is the unitary external forces,

$\left(\frac{\partial f}{\partial t}\right)_{\text{col}}$ – represents the collisional term.

Fluid flow is determined by numerically solving Equation 5 on a binary grid. The grid is usually defined as a three-dimensional matrix of logical numbers, e.g., a value of 1 characterizes a grid point of the solid body and 0 values mean that the point is a part of the pore space.

The algorithm to solve Equation 5 covers two main steps (BHATNAGAR et al. 1954):

a) streaming processes; and

b) collision process, which is the mathematically critical step.

Characteristic for the LBM is that streaming occurs only in discrete directions. Two numbers, define the variant of the LBM model: the dimensionality (e.g. D3) and the number of directions (e.g. Q27). Thus, D3Q27 describes a model in three-dimensions where the lattice gas can move in 27 directions. The most popular LBM variants are D2Q9, D3Q15, D3Q19 and D3Q27.

Knowing the distribution function (f) in each i^{th} direction allows to calculate the macroscopic density and the macroscopic velocity of the lattice gas using:

$$\rho = \sum_{i=0}^{n_i} f_i e_i \tag{6}$$

and

$$v = \frac{1}{\rho} \sum_{i=0}^{n_i} f_i e_i \tag{7}$$

where:

r – lattice gas density,

v – lattice gas velocity,

e_i – direction vectors,

n_i – the number of the space directions in the model.

The calculated flow velocities by the LBM are used to compute the hydraulic tortuosity according to the Equation 2.

We calculated creeping flow in the Lattice Boltzmann Method making use of the Palabos numerical code (Palabos Home 2017). We applied a D3Q27 model with periodic boundary condition in the main direction flow. In the other directions (X and Y), we applied the bounce-back boundary condition to mimic

the no flow boundaries. The unitary external force (Eq. 5) responsible for the movement of the lattice gas were set to 0.0, 0.0 and 0.0001 lattice units [lu] in X, Y and Z direction at all nodes in the pore space. The relaxation time was constant and simulation results were recorded after 1000, 2000, 4000, 8000, 16 000 and 32 000 iterations.

Geometry Conversion

Using DEM generated geometries for LBM calculation requires a conversion step since both methods rely on different geometry conceptualizations. The vector geometry description of the grain objects in the DEM needs to be transformed into an LBM structured binary grid as summarized in Figure 1.

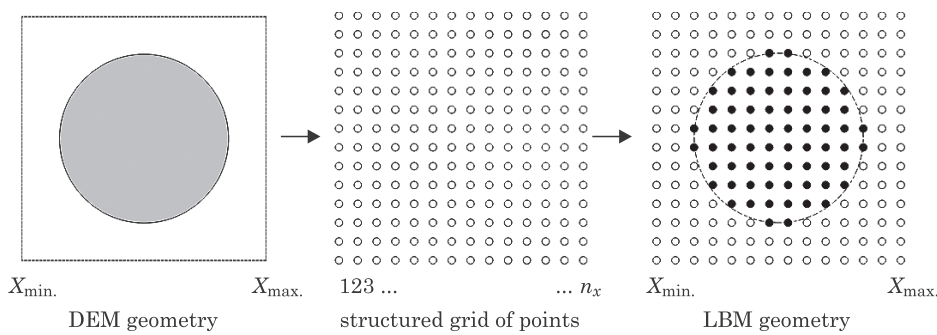

Fig. 1. Schema of geometry conversion between DEM and LBM

We implemented a Fortran code to convert the DEM geometry to an LBM binary structure matrix of 0's and 1's.

Two types of structural grids may be distinguished: node-centred and cell-centred grids. Both kinds of grids may be conveniently visualised by ParaView (ParaView Home 2020), MayaVi (MayaVi Home 2020) or other similar software. We follow the second approach given that grain centres can directly be interpreted as points in the LBM grid. As a consequence, the number of cells equals the number of points simplifying the implementation of the LBM.

Given the geometric parameters, the LBM grid value is specified as 1 (solid) if a sphere is overlapping the grid coordinate, and otherwise 0 (void space), as visualized in Figure 2. The total number of solid points representing a grain is a function of the LBM grid resolution. It is characterized by the number of points per direction (n_x, n_y and n_z). A sufficient resolution of grains is relevant for computational accuracy as outlined by (WANG 2014), and further discussed in section *Geometry conversion for a LBM model*.

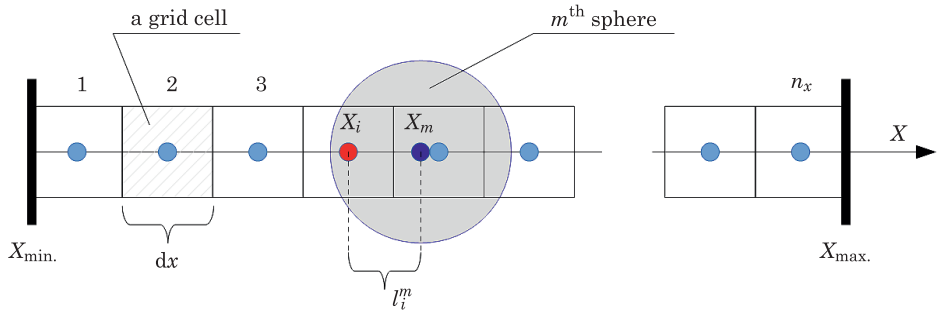

Fig. 2. Converting the geometry from DEM coordinates to a LBM grid for a selected space direction

Path Tracking Method

We calculate geometrical tortuosity using the Path Tracking Method (PTM), developed by Sobieski (SOBIESKI 2009, SOBIESKI et al. 2016a). The numerical method calculates the lengths of paths in granular beds based on the geometrical parameters of the grains. The length of a path across the domain is the sum of the unitary lengths calculated inside local tetrahedral structures (Fig. 3). We performed calculation with the PathFinder code (a freely available implementation of the PTM method). Details on the PTM can be found in the PathFinder Users' Guide (SOBIESKI, LIPIŃSKI 2016).

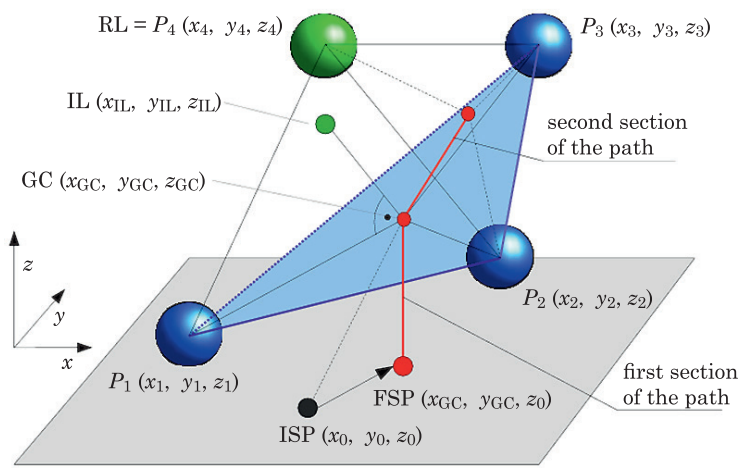

Fig. 3. Schema of the tetrahedral structure used in the Path Tracking Method; meaning of abbreviations: ISP – Initial Starting Point (starting point of calculation), FSP – Final Starting Point (starting point of the path), GC – gravity center of the triangle formed by particles P_1, P_2 and P_3, IL – Ideal Location (predicted centre of particle P_4 forming the tetrahedral structure), RL – Real Location (actual centre of particle P_4)

Knowing the path length within the granular domain allows to calculate the geometric tortuosity of that path based on Equation 1. The procedure is repeated for multiple starting points to calculate the average tortuosity value as the domain tortuosity. The algorithm allows to calculate the tortuosity independent of the resolution (SOBIESKI 2016).

We applied the method to 25×25 Initial Starting Points on a regular grid. Doing so, we arrived at a domain tortuosity as average over 625 paths. Some of these paths coincide when initial starting points end up in the same trajectory. SOBIESKI et al. (2012) found that this effect is not insignificant. Furthermore, he pointed out that 25 individual paths of fully distinct trajectories are sufficient to obtain a representative value of the tortuosity. Representative value here means that the average does not change with increasing number, in line with the concept of represenative elementary volumes (REV) (BEAR 1972).

We calculate the porosity of the specific virtual bed using the PathFinder code. The analytically determined value of 0.5832 equals the value reported by the YADE code with a relative error of 0.03%.

Results and Discussion

Virtual bed

The 3D realization of a porous medium structure with 50 grains is visualized in Figure 3. The virtual bed was created using YADE open source numerical code (ŠMILAUER et al. 2017), which uses the Discrete Element and the Radius Expansion Method as described in section *Discrete Element Method*. Details on the procedure can be found in (SOBIESKI et al. 2016a, 2016b).

Grains have a size distribution with an average diameter of $d = 5.9$ mm and standard deviation of $\sigma = 0.051$ mm (Fig. 4). The porosity of the bed is $\phi = 0.583$, based on geometrical calculations. The size of the domain and number of particles

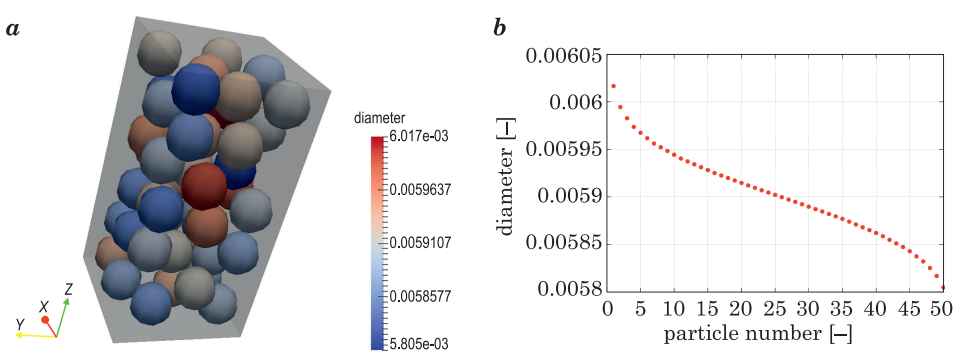

Fig. 4. 3D view (*a*) and particle size distribution (*b*) of the generated virtual bed

was chosen in balance between numerical accuracy and the computational limitations. The slight deviation of the average diameter from the starting value is a results of the growing process within the Radius Expansion Method. This aspect, however, does not impact the results of this study.

Geometry conversion for a LBM model

We prepared 8 LBM grid resolution of the virtual bed of $n_x \times n_y \times n_y$ (with n being the total number of grid points): $32 \times 32 \times 64$ ($n = 65\,536$), $64 \times 64 \times 128$ ($n = 524\,288$), $96 \times 96 \times 192$ ($n = 1\,769\,472$), $128 \times 128 \times 256$ ($n = 4\,194\,304$), $160 \times 160 \times 320$ ($n = 8\,192\,000$), $192 \times 192 \times 384$ ($n = 14\,155\,776$), $224 \times 224 \times 448$ ($n = 22\,478\,848$) and $256 \times 256 \times 512$ ($n = 33\,554\,432$). Figure 5*a* shows the virtual bed and its equivalent in a form of the lattice grid in coarse resolution. Figure 5*b* a cross section shows how the particle surface is approximated by grid cells.

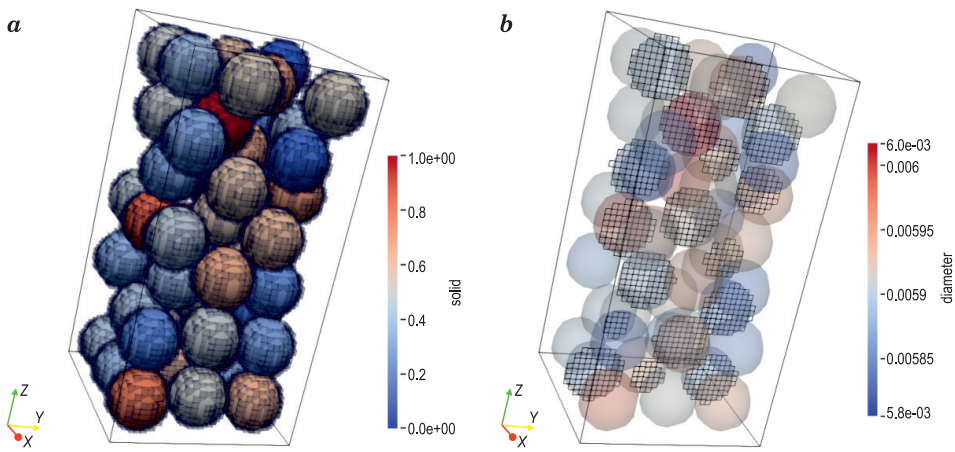

Fig. 5. Example of the LBM grid generated for the virtual bed with a resolution of $32 \times 32 \times 64$: *a* – full view, *b* – cross-section in *YZ* plane

The higher the resolution of a single particle in the LBM grid, the higher are the computational cost for the grid conversion. Figure 6 provides an example for a sphere in LBM grid resolutions of $32 \times 32 \times 32$; $96 \times 96 \times 96$ and $160 \times 160 \times 160$ points.

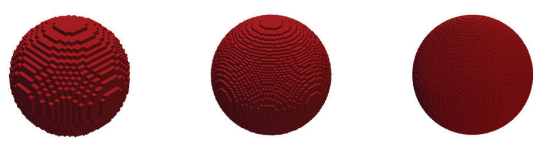

Fig. 6. A simple sphere converted to LBM grid with different resolutions

According to WANG (2014), the radius of each sphere should be at least resolved by ten lattice nodes. All except the smallest of our LBM grids fulfil this condition with lattice nodes per radius of 5 (Fig. 5*b*), 10, 15, 20, 25, 30, 35 and 40, respectively.

Figure 7 summarizes the conversion time (t_c) as function of the grid point number. Time increases linearly $t_c = ax + b$ with a slope of $a = 0.000154$ and $b = 0$. At high resolutions conversion times are up to hours. This aspect becomes critical when applying the method in hybrid methods with feedback loops for cases with changes in the solid phase.

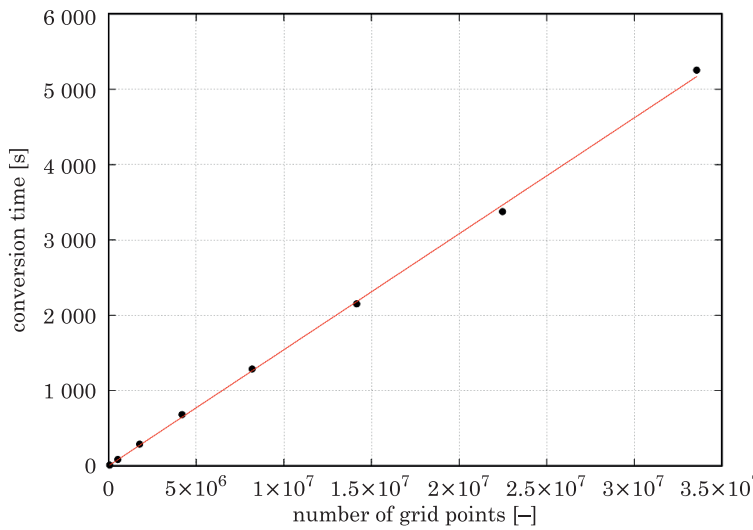

Fig. 7. Conversion time in function on grid resolution

We check the influence of the grid resolution on the LBM geometry by calculating a LBM porosity as

$$\phi_{\mathrm{LBM}} = \frac{n_0}{n_x n_y n_z} \tag{8}$$

where:

n_0 – the number of grid points belonging to the porous space of the granular bed (denoted by 0 in the geometry matrix) [-],

$n_x n_y n_z$ – the total number of points in the grid [-].

Figure 8 shows the LBM porosity as function of resolution. The LBM porosity decreases approaching an asymptotic value. The trend can be fitted to the functional relationship:

$$\phi_{\mathrm{LBM}} = \frac{ax + b}{cx + d} \tag{9}$$

with coefficients a, b, c and d equal to 1.17325, 0.141114, 2.01073 and 0.131859, respectively.

The LBM porosity is greater than the geometrical porosity of the DEM model, clearly overestimating the porosity of the porous body. However, the relative errors decrease with increasing grid resolution and do not exceed a few percent as shown in the subplot of Figure 8. The relative errors between the LBM porosity and the reference porosity are a good indicator for the minimum required grid resolution, with an acceptable level of about 1% (Fig. 8).

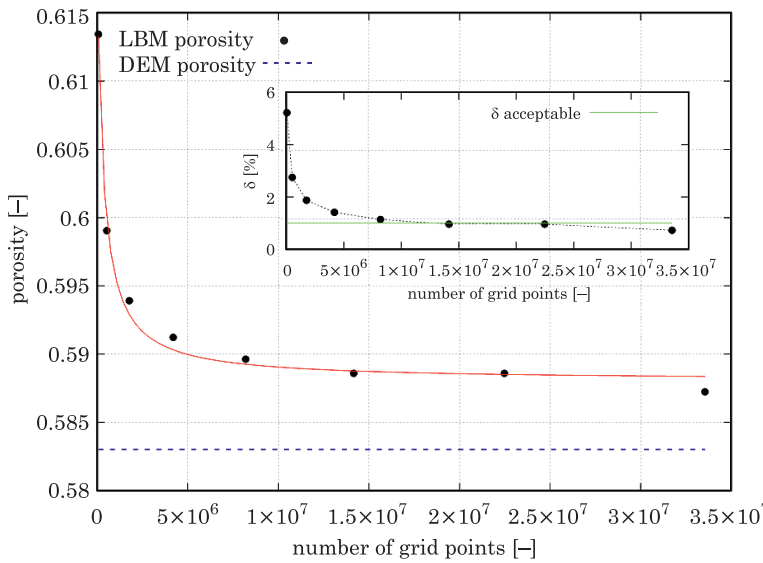

Fig. 8. LBM porosity as function of the grid resolution for cases 1–8.

LBM simulation

We calculated the velocity distribution in the LBM grids using the Palabos numerical code (Palabos Home 2017) with computational specifications outlined in section *Lattice Boltzmann Method*. Figure 9 shows the virtual bed, the converted LBM grid (with reduced resolution of points), the distribution of the lattice gas density (being close to one in the pore space and zero inside the spheres) and the distribution of the velocity field.

Figures 10 and 11 displays the dependency of the average and maximum lattice gas density to the number of grid nodes and the number of iterations. Both show

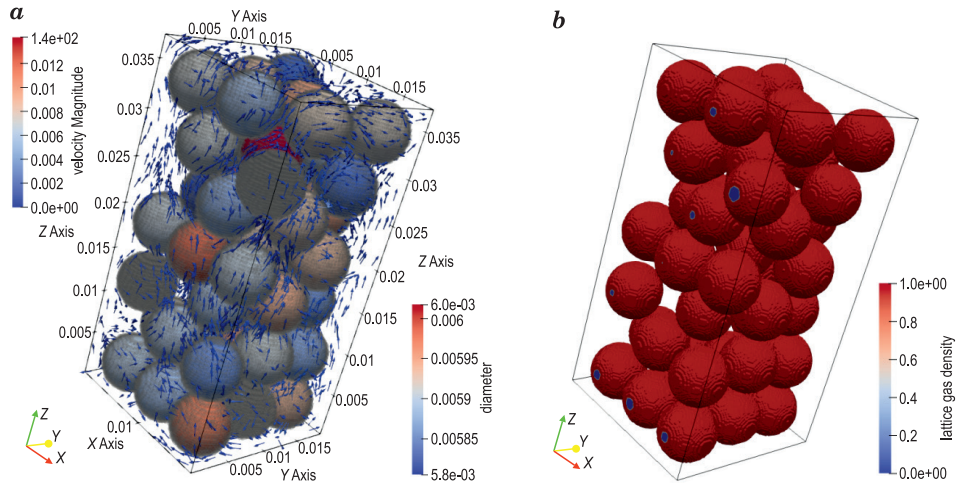

Fig. 9. Results of LBM flow field calculations for the grid of 128×128×256 (after 16 000 iterations): *a* – velocity field, *b* – binary form of the bed geometry

non-linear relationships. We focus on the lattice gas density as central quantity from which all other parameters, such as velocity or pressure can be inferred.

Figure 10 shows that a minimum number of iterations is needed to obtain a steady state for small grid resolutions. For the grids containing 65 536 and 524 288 (65 536×8) nodes approximately 2000 and 16 000 (2000×8) are need. Thus, the minimum number of iterations depends linearly on the grid resolution. Obtaining steady state for large grids is, in practice, strongly limited by the massive calculation times. Following the trend, the required simulation time (on the same computer) is about 135 days for the largest grid. This value was estimated on the basis of data obtained for the grid 32×32×64 (65 536 nodes) and 16 000 iterations, where the calculation time was equal to 34 026 s. In turn, the number of nodes for the grid resolution 224×224×448 (22 478 848 nodes) is 343 times greater. Assuming a linear trend, the calculation time needed for performing the same number of iterations should be 343 times longer, thus about 135 days.

In Figure 11 shows a comparison for the maximum values of the lattice gas. Again, values increase with the grid resolution. The maximum values of the lattice gas velocity may be even 15 times greater than the average ones.

Figure 12 displays the average velocity as function of grid resolution and the number of iterations. The deviation of results for less than 4000 iterations suggests that the required minimum number of iterations is about 8000, independent of the grid resolution. Increasing the iterations beyond 8000 does not change the velocity for the same grid resolution. However, velocities differ between grid resolution, with higher values for denser grids.

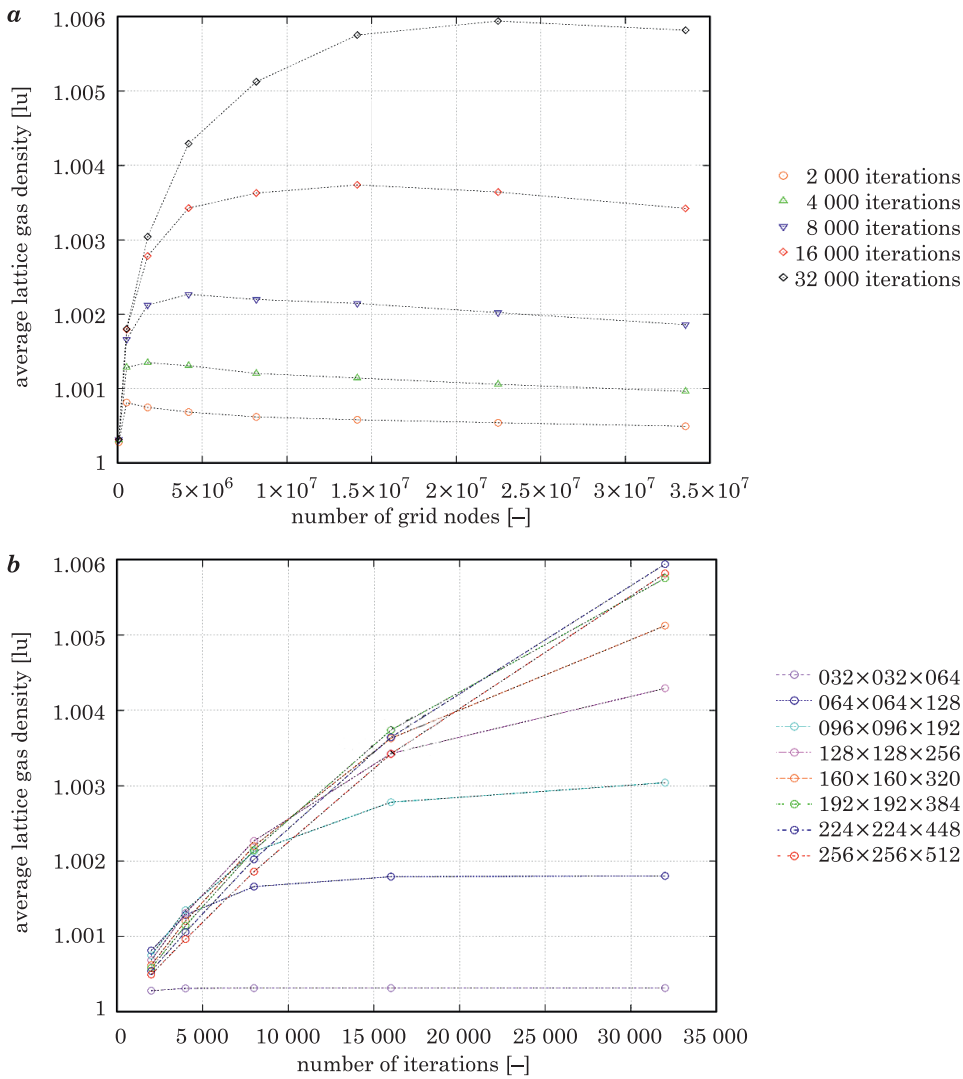

Fig. 10. Average density of the lattice gas as a function of the grid resolution (*a*) and the number of iterations (*b*)

Table 2 summarizes average velocities and relative errors compared to the highest resolution (256×256×512) with 32 000 iterations. The small average velocity for the lowest grid resolution clearly shows that it is too coarse, which is in line with the conclusion of WANG (2014) regarding the resolution of solid particle in the LBM grid.

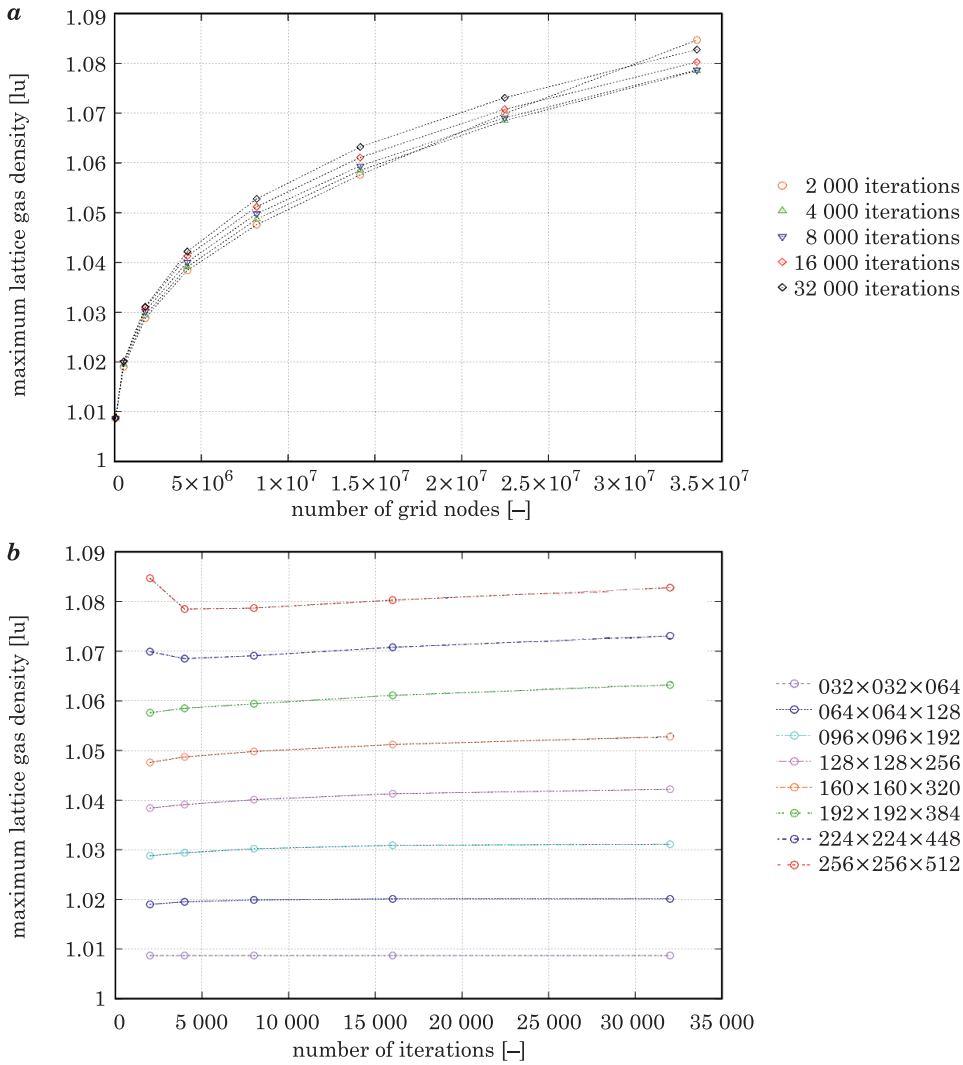

Fig. 11. Maximum value of the lattice gas density as a function of the grid resolution (*a*) and the number of iterations (*b*)

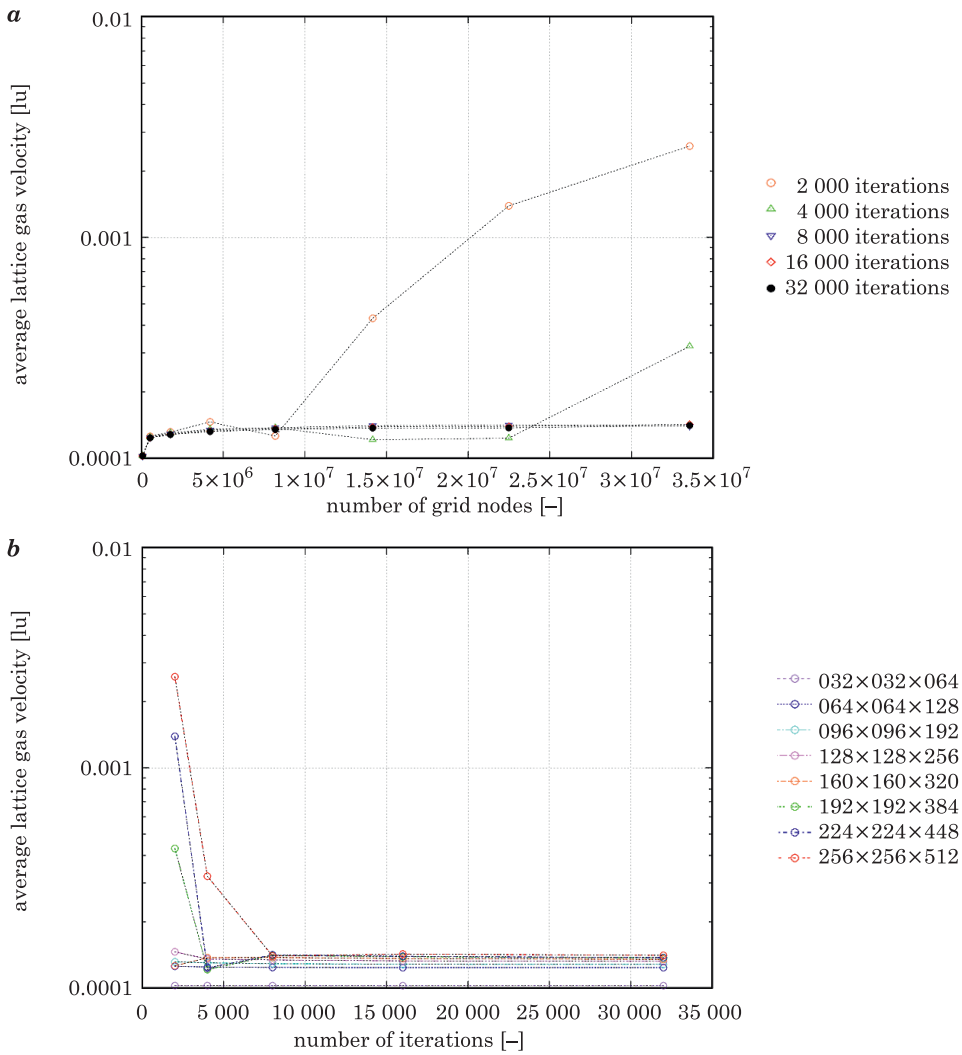

Fig. 12. Average velocity of the lattice gas density as a function of the grid resolution (*a*) and the number of iterations (*b*)

Table 2

Average lattice gas velocities v_{ave} and relative errors δ (relative to highest resolution) for 32 000 iterations

Case No.	n [-]	v_{ave} [lu]	δ [%]
1	65 537	1.0243E-04	27.16
2	524 289	1.2372E-04	12.02
3	1 769 473	1.2795E-04	9.02
4	4 194 305	1.3200E-04	6.14
5	8 192 001	1.3487E-04	4.09
6	14 155 777	1.3694E-04	2.62
7	22 478 849	1.3723E-04	2.41
8	33 554 432	1.4063E-04	0.00

Figure 13 shows the hydraulic tortuosity calculated from the LBM results using Equation 2. All cases give physically acceptable values, i.e., $\tau > 1$. We see that values stabilize for 8000 iterations and more, independent of the grid resolution. This supports the previous finding that 8000 is the required minimum number of iterations.

The hydraulic tortuosity at sufficient iterations differs among grid resolutions, although only slightly for higher resolutions. The asymptotic value ranges around 1.556. Assuming that the result obtained for the highest grid resolution and 32 000 iterations provides the most exact value, we can determine the relative errors for other cases (at 32 000 iterations) as: 0.74%, 0.84%, 1.08%, 2.14%, 4.09%, 7.87% and 14.16% for cases 7 to 1, respectively.

In addition to our hydraulic tortuosity results, we have shown the result obtained by WANG (2014) in Figure 13. We consider the domain size to be one reasons for deviation between our results and that of Wang as he used a larger porous structure, thus the boundaries affect the results less. In our model all spheres are located inside the domain, giving that the porosity is higher near the walls. Thus, preferential pathways with higher velocities are formed (Fig. 14), leading to an overestimation of tortuosity.

To explore the effect of the boundaries, we recalculated the tortuosity considering only velocities within the domain (Fig. 14*b*) within a distance of 10% of the domain size from the outer boundary. Figure 15 shows the hydraulic tortuosity as function of the LBM settings for the reduced amount of velocity values. Generally, the tortuosity decreases. For the highest resolution by about 4% from 1.556 to 1.49. Analogously, in the range of 4% for the other cases. However, the calculated value of hydraulic tortuosity stays high, indicating that the method of determining tortuosity independent of the pathways by relating fluid velocities might be error prone for high porosities.

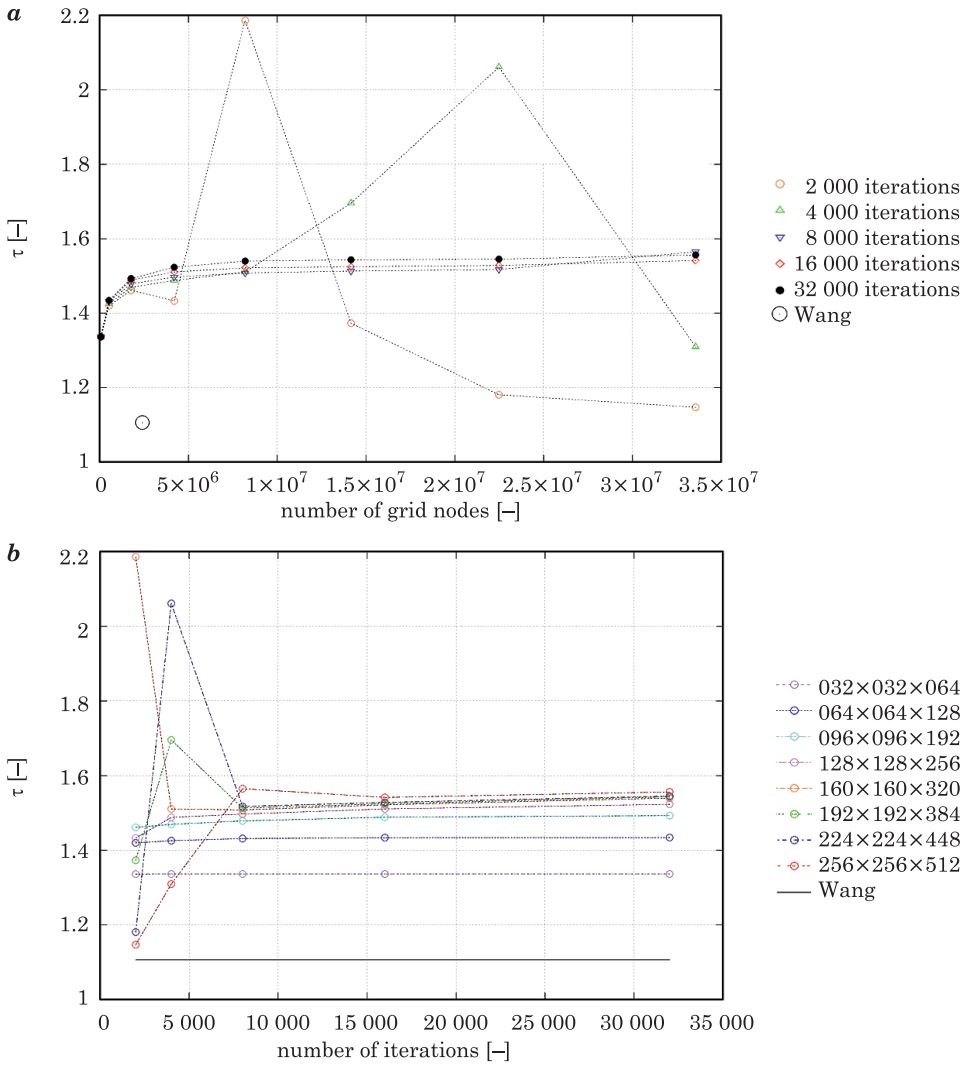

Fig. 13. Hydraulic tortuosity as function of the grid resolution (*a*) and the number of iterations (*b*)

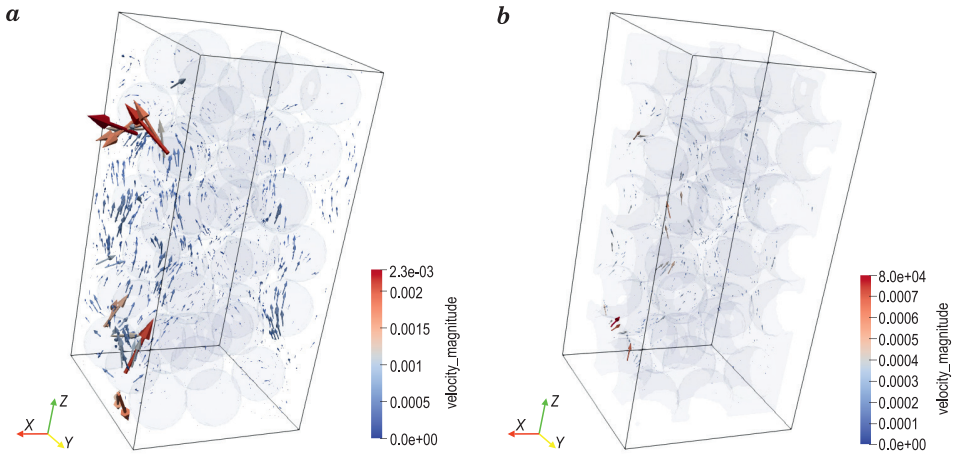

Fig. 14. Visualisations of the velocity field for the grid 64×64×128 and 32 000 iterations taking all value into account (*a*) and cutting off boundary effects (*b*)

Our results show that grid resolution in LBM has an impact on the calculated hydraulic tortuosity. Thus, we cannot agree with KOPONEN et al. (1996) who found that for a given obstacle configuration the tortuosities calculated with different lattice resolutions were close to each other. The same conclusion was given by NABOVATI and SOUSA (2007), stating that the effect of the domain resolution is negligible in the range examined. These conclusions were developed on the basis of 2D simulations and may not be applicable for 3D geometries. This is also supported by the results of Wang who stated that the radius of the sphere should not be less than ten lattices. We see that tortuosity differences become very small when the grid resolution and the number of iterations increase. However, both model parameters are subject to the specific case setting and needs to be determined individually, which takes additional time.

PTM calculations

In the second stage, we used the Path Tracking Method to determine the geometrical tortuosity of the granular bed (section *Path Tracking Method*). Figure 16 shows one calculated path. Figure 17 visualizes the tortuosity field for the 625 individual starting points. The average value (τ_{ave}) is 1.185 which is 7.14% higher than the tortuosity of Wang (1.106). Figure 18 summarizes the individual tortuosity values of all paths. Additionally, it contains values for two characteristic cases:

– the grid resolution 32×32×64 (Fig. 10*b*),
– the highest grid resolution 256×256×512.

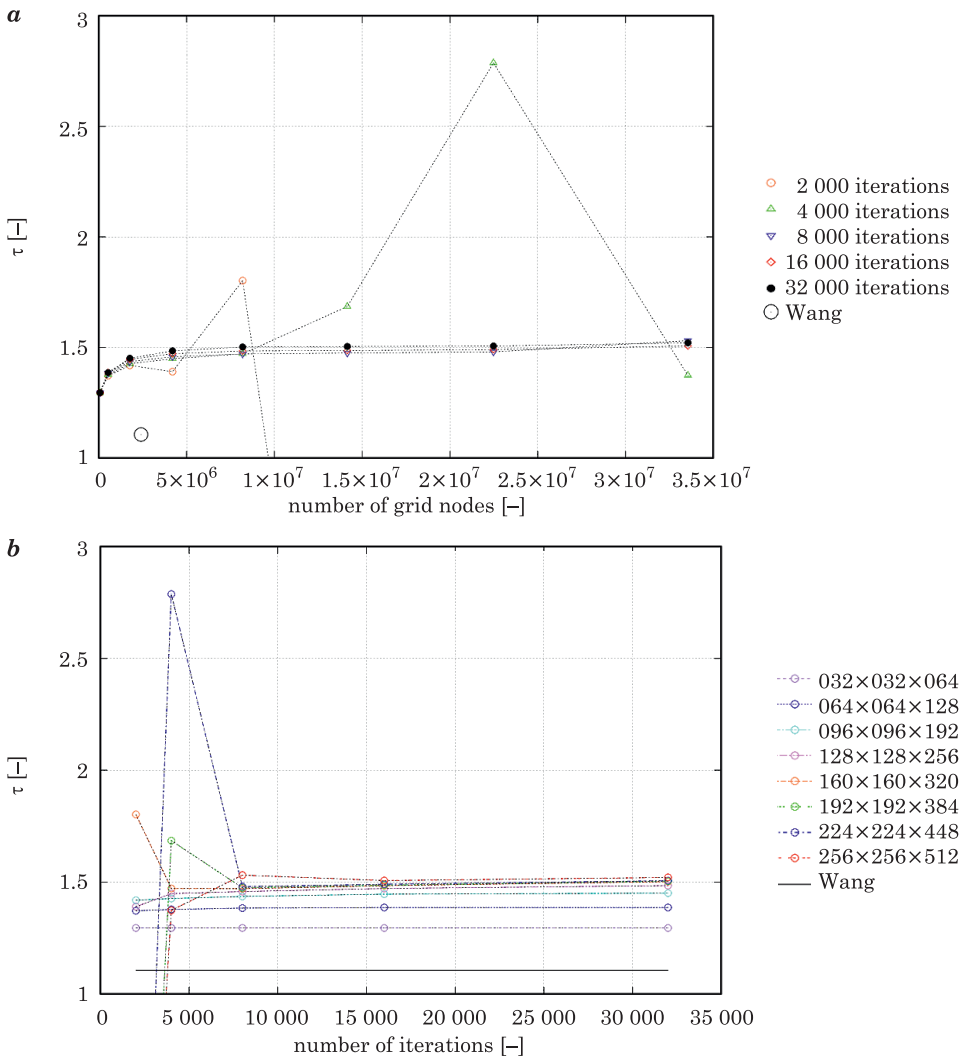

Fig. 15. Hydraulic tortuosity as function of the grid resolution (*a*) and the number of iterations (*b*) for simulated velocities in the inner domain

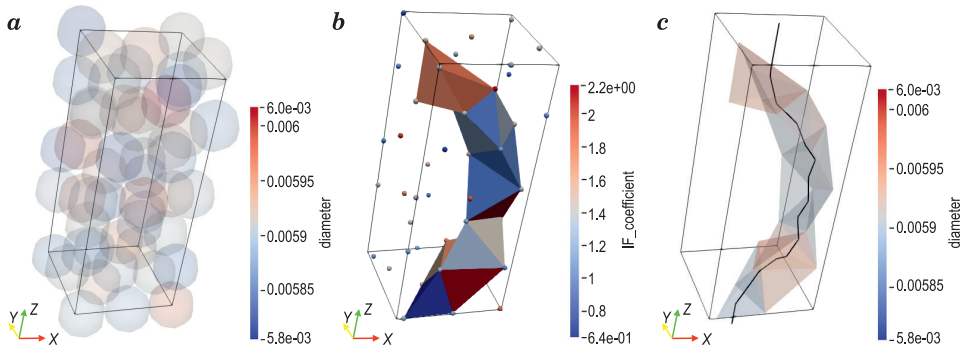

Fig. 16. Visualisation of the granular bed (*a*), tetrahedral structures used in the Path Tracking method (dots represent the spheres centres) (*b*) and the final path (*c*)

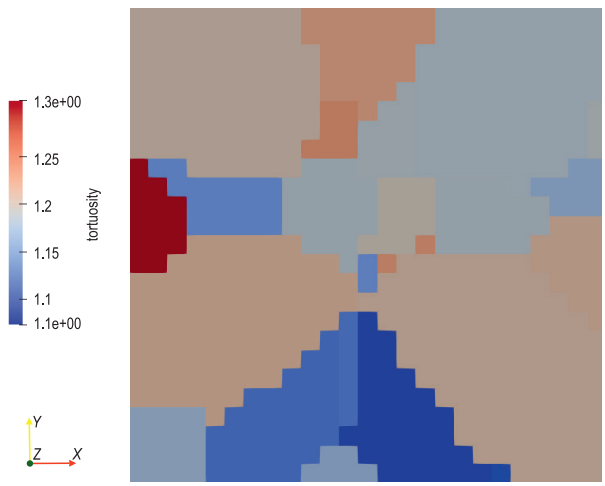

Fig. 17. Tortuosity as function of the starting point coordinates for the 625 individual locations

In both cases the number of iterations is equal to 32 000. The tortuosities obtained with LBM are clearly higher than for the others cases. Thus, it remains open which value represent tortuosity best in the LBM approach. Potential factors for improvement might be a bigger domain size, higher lattice resolution and/or more iterations.

Figures 17 and 18 show large areas of equal tortuosity values. These starting points end up in identical trajectories. They are represented by the same Final Starting Point (see Fig. 3). The sizes and shapes of these areas depends on the local arrangement of particles. For details on tortuosity fields, the reader is referred to SOBIESKI (2016).

The calculation time of the 625 individual path lengths was very short, in the order of a few minutes. Figure 19 shows the individual calculation times

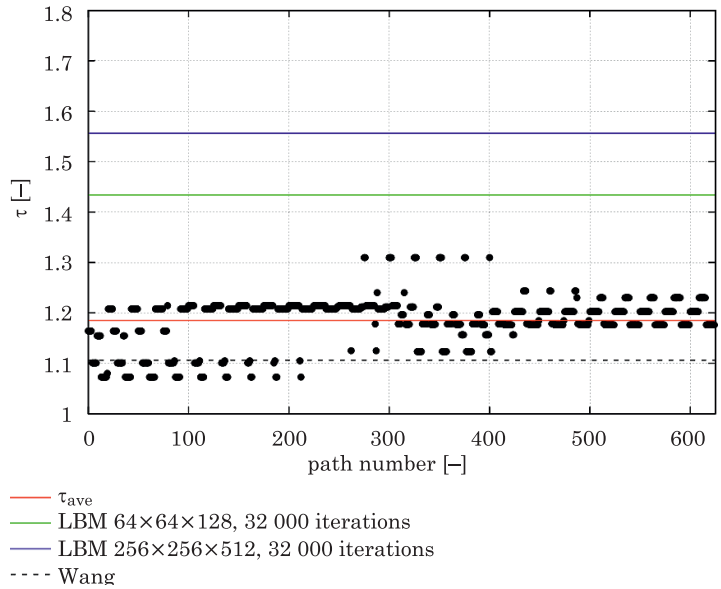

Fig. 18. Individual tortuosity values for the 625 initial starting points

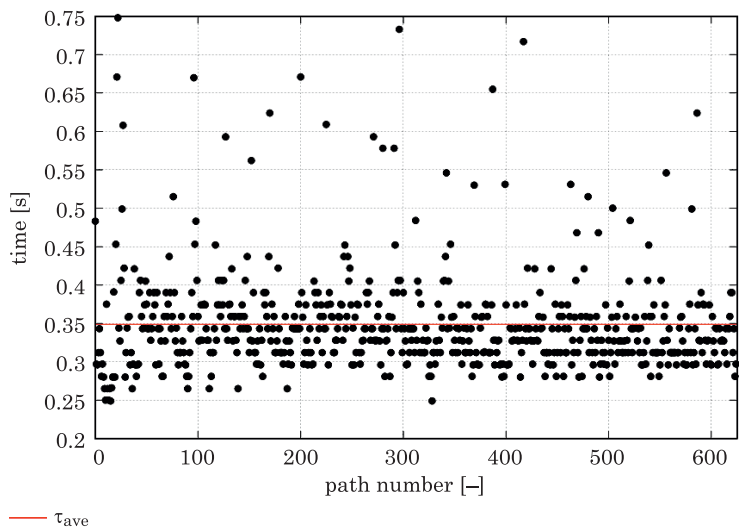

Fig. 19. Calculation times of the individual path length with the PTM

summing up to about 218 s. It can be seen that calculation times differ depending on the Initial Starting Point, which differences up to a factor of 3. Compared to the LBM simulations, this is 10 times faster for the smallest grid resolution and 2000 iterations. For the high grid resolution of 256×256×512 and 32 000 iterations, the ratio equals about 83 700. This illustrates a major advantage of the PTM approach.

Another benefit of the PTM is the spatial resolution of the individual tortuosity values. Obtaining a distribution of tortuosities for granular beds allows to perform detailed analysis of flow field specifications and statistical analysis.

Summary and Conclusions

We performed a comparison of two numerical methods to calculate tortuosity of granular beds using generated 3D media. We applied the Lattice Boltzmann Method (LBM) to compute hydraulic tortuosity based on the ratios of flow velocities and also used Path Tracking Method (PTM) which directly calculates geometric tortuosity. For both methods, we investigated computation times as well as the quality of tortuosity values given data resolution.

Table 3 summarizes the main features of both methodologies. In particular, this study has shown that:

– The resolution of the LBM grid plays a critical role. It affects the conversion time (linearly), the actual porosity, the calculation time (linearly), and the calculated velocity values. The density and the velocity of the lattice gas depend non-linearly on LBM grid.

– The number of iterations performed during the LBM simulations is important. Both, average and maximum lattice gas density change non-linearly. Thus, other quantities are affected as well. Our results suggest a minimum number of 8000 iterations.

– The Lattice Boltzmann Method requires large computing power, particularly given a accurate grid resolution and sufficient iteration steps. This hampers its use on standard personal computers. Parallel computing is a prerequisite for analysing more realistic porous beds where larger domain sizes and denser particle packings are encountered.

– The application of the LBM requires a quality check on resolutions and iteration steps. Average values of the lattice gas density and the velocity should be compared for different settings. However, for repeated investigations on similar geometries (e.g., only changing the number of objects in the DEM) one test is sufficient.

– The Path Tracking Method is beneficial as it is fast and easy to implement. It is free from conversion requirements. The only resolution dependency refers

to the number of initial starting points. However, a small number is sufficient to properly determine the domains tortuosity from individual pathways.

– PTM offers great advantage over any indirect way of calculating hydraulic tortuosity using flow velocities (independent of the specific method used) as it circumvents the requirement to calculate the velocity field in the pore space of the media.

Table 3

Summary and comparison of features of Lattice Boltzmann Method (LBM) and the Path Finder Method (PFM) for calculating tortuosity starting from grain bed geometry (defined by geometric parameters)

Feature	LBM	PTM
Geometry conversion	required pre-processing step; increases computation time; requires additional software for geometry conversion	not required
Porosity	depends on grid resolution; may also depend on conversion algorithm used	analytically calculated
Tortuosity	calculated indirectly; depend on multiple factors as grid resolution, iterations, choice of LBM model, numerical model settings	calculated from geometry; directly related to flow path, provides individual values within domain
Computational demand	very high (for calculations and visualisation)	very low
Computation time	very long	very short (depending on number of starting points)
Software	Pre-processing tool; Lattice Boltzmann solver; postprocessing tool	Path Finder (no further software required)

The publication was written during the first author's internship at Utrecht University, co-financed by the European Union under the European Social Fund (Operational Program Knowledge Education Development), carried out in the project Development Program at the University of Warmia and Mazury in Olsztyn (POWR.03.05. 00-00-Z310/17).

References

AFKHAMI M., HASSANPOUR A., FAIRWEATHER M., NJOBUENWU D.O. 2015. *Fully coupled LES-DEM of particle interaction and agglomeration in a turbulent channel flow*. Computers and Chemical Engineering, 78: 24-38.

AL-ARKAWAZI S., MARIE C., BENHABIB K., COOREVITS P. 2017. *Modeling the hydrodynamic forces between fluid-granular medium by coupling DEM-CFD*. Chemical Engineering Research and Design, 117: 439-447.

BEAR J. 1972. *Dynamics of Fluids in Porous Media*. Courier Dover Publications, New York.

BHATNAGAR P.L., GROSS E.P., KROOK M. 1954. *A model for collisional processes in gases I: small amplitude processes in charged and neutral onecomponent system*. Physical Review, 94(3): 511-524.

CARMAN P.C. 1937. *Fluid Flow through Granular Beds*. AIChE, 15: 150.

CATALANO E. 2012. *A pore- coupled hydromechanical model for biphasic granular media*. Ph.D. Thesis, Grenoble University, France.

CHEN F. 2009. *Coupled Flow Discrete Element Method Application in Granular Porous Media using Open Source Codes*. Ph.D. Thesis, University of Tennessee, Knoxville, USA.

CIESZKO M. 2009. *Description of anisotropic pore space structure of permeable materials based on Minkowski metric space*. Arch. Mech., 61(6): 425-444.

CIESZKO M., KRIESE W. 2006. *Description of tetragonal pore space structure of porous materials*. Arch. Mech., 58(4-5): 477-488.

CUNDALL P.A., STRACK O.D. 1979. *A discrete element model for granular assemblies*. Géotechnique, 29: 47-65.

DUDA A., KOZA Z., MATYKA M. 2011. *Hydraulic tortuosity in arbitrary porous media flow*. Physical Review, E, 84: 036319.

ERATH C. 2010. *Coupling of the Finite Volume Method and the Boundary Element Method*. Ph.D. Thesis, University Ulm, Germany.

FENG Y.T., HAN K., OWEN D.R.J. 2007. *Coupled lattice Boltzmann method and discrete element modelling of particle transport in turbulent fluid flows: Computational issues*. International Journal for Numerical Methods in Engineering, 72: 1111-1134.

Free Software Foundation. 2019. https://www.fsf.org/ (access: 10.02.2020).

GALINDO-TORRES S.A. 2013. *A coupled Discrete Element Lattice Boltzmann Method for the simulation of fluid-solid interaction with particles of general shapes*. Computer Methods in Applied Mechanics and Engineering, 265: 107-119.

GHAREDAGHLOO B., PRICE J.S., REZANEZHAD F., QUINTON W.L. 2018. *Evaluating the hydraulic and transport properties of peat soil using porenetwork modeling and X-ray micro computed tomography*. Journal of Hydrology, 561: 494-508.

KOMORÓCZI A., ABE S., URAI J.L. 2013. *Meshless numerical modeling of brittle – viscous deformation: first results on boudinage and hydrofracturing using a coupling of discrete element method (DEM) and smoothed particle hydrodynamics (SPH)*. Computational Geosciences, 17(2): 373-390.

KOPONEN A., KATAJA M., TIMONEN J. 1996. *Tortuous flow in porous media*. Phys. Rev. E, 54: 406.

KOPONEN A., KATAJA M., TIMONEN J. 1997. *Permeability and effective porosity of porous media*. Phys. Rev. E, 56: 3319.

LINDNER S. 2015. *SiLibeads Glass beads Type S, Microglass beads*. Product Data Sheet, Version V13. http://www.tecmos.com/wp-content/uploads/2018/05/SiLibeads-Type-S.pdf.

MAHABADI O.K. LISJAK A., HE L., TATONE B.S.A., KAIFOSH P., GRASSELLI G. 2016. *Development of a New Fully-Parallel Finite-Discrete Element Code: Irazu*. ARMA, 16: 516.

MAREK M. 2014. *CFD modelling of gas flow through a fixed bed of Raschig rings*. Journal of Physics, Conference Series, 530: 012016.

MARKAUSKAS D., KRUGGEL-EMDEN H., SIVANESAPILLAI R., STEEB H. 2017. *Comparative study on mesh-based and mesh-less coupled CFD-DEM methods to model particle-laden flow*. Powder Technology, 305: 78-88.

MARKL M. 2015. *Numerical Modeling and Simulation of Selective Electron Beam Melting Using a Coupled Lattice Boltzmann and Discrete Element Method*. Ph.D. Thesis, Friedrich-Alexander-University Erlangen-Nuremberg, Germany.

Mayavi: 3D scientific data visualization and plotting in Python. 2020. MayaVi. https://docs.enthought.com/mayavi/mayavi/ (access: 10.02.2020).

NABOVATI A., SOUSA A.C.M. 2007. *Fluid Flow Simulation in Random Porous Media at Pore Level Using Lattice Boltzmann Method*. In: *New Trends in Fluid Mechanics Research*. Eds. F.G. Zhuang, J.C. Li. Springer, Berlin, Heidelberg.

NORDBOTTEN J.M. 2014. *Finite volume hydromechanical simulation in porous media*. Water Resources Research, 50(5): 4379-4394.

Palabos. 2020. Universite de Geneve. http://www.palabos.org/ (access: 10.02.2020).

ParaView. 2020. http://www.paraview.org/ (access: 10.02.2020).

QIU L.-C. 2015. *A Coupling Model of DEM and LBM for Fluid Flow through Porous Media*. Procedia Engineering, 102: 1520-1525.

ROJEK J. 2007. *Multiscale analysis using a coupled discrete/finite element model*. Interaction and Multiscale Mechanics, 1(1): 1-31.

SAKAI M. 2016. *How Should the Discrete Element Method Be Applied in Industrial Systems?* KONA Powder and Particle Journal, 33: 169-178.

SAOMOTO H., KATAGIRI J. 2015. *Direct comparison of hydraulic tortuosity and electric tortuosity based on finite element analysis*. Theoretical and Applied Mechanics Letters, 5(5): 177-180.

SOBIESKI W. 2009. *Calculating tortuosity in a porous bed consisting of spherical particles with known sizes and distribution in space*. Research report 1/2009, Winnipeg, Canada.

SOBIESKI W. 2016. *The use of Path Tracking Method for determining the tortuosity field in a porous bed*. Granular Matter, 18: 72.

SOBIESKI W., DUDDA W., LIPIŃSKI S. 2016a. *A new approach for obtaining the geometric properties of a granular porous bed based on DEM simulations*. Technical Sciences, 19(2): 165-187.

SOBIESKI W., LIPIŃSKI S. 2016. *PathFinder User's Guide*. University of Warmia and Mazury, Olsztyn.

SOBIESKI W., LIPIŃSKI S., DUDDA W., TRYKOZKO A., MAREK M., WIĄCEK J., MATYKA M., GOŁEMBIEWSKI J. 2016b. *Granular porous media*. University of Warmia and Mazury, Olsztyn.

SOBIESKI W., ZHANG Q., LIU C. 2012. *Predicting Tortuosity for Airflow Through Porous Beds Consisting of Randomly Packed Spherical Particles*. Transport Porous Med., 93(3): 431-451.

SRIVASTAVA S., YAZDCHI K., LUDING S. 2012. *Mesoscale dynamic coupling of finite- and discrete-element methods for fluid-particle interactions*. Philosophical Transactions of the Royal Society A, 372(2021): 1-18.

STRÁNSKÝ J., JIRÁSEK M. 2012. *Open source FEM-DEM coupling*. 18th International Conference Engineering Mechanics, Svratka, Czech Republic, May 14-17, Paper no 18, p. 1237-1251.

SUN W.C., KUHN M.R., RUDNICKI J.W. 2013. *A multiscale DEM-LBM analysis on permeability evolutions inside a dilatant shear band*. Acta Geotechnica, 8(5): 465-480.

ŠMILAUER V., CATALANO E., CHAREYRE B., DOROFEENKO S., DURIEZ J., DYCK N., ELIÁŠ J., ER B., EULITZ A., GLADKY A., GUO N., JAKOB CH., KNEIB F., KOZICKI J., MARZOUGUI D., MAURIN R., MODENESE CH., SCHOLTÈS L., SIBILLE L., STRÁNSKÝ J., SWEIJEN T., THOENI K., YUAN CH. 2020. *Yade Documentation*. 2nd Edition, after Release 2020-04-30.git-c3696f2. https://yade-dem.org/doc/Yade.pdf (access: 10.02.2020).

TRYKOZKO A., PESZYNSKA M., DOHNALIK M. 2016. *Modeling non-Darcy flows in realistic pore-scale proppant geometries*. Computers and Geotechnics, 71: 352-360.

VILLARD P., CHEVALIER B., LE HELLO B., COMBE G. 2009. *Coupling between finite and discrete element methods for the modelling of earth structures reinforced by geosynthetic*. Computers and Geotechnics, 36(5): 709-717.

WANG P. 2014. *Lattice Boltzmann Simulation of Permeability and Tortuosity for Flow through Dense Porous Media*. Math. Prob. Eng., 694350.

WIDULIŃSKI Ł., KOZICKI J., TEJCHMAN J. 2009. *Numerical Simulations of Triaxial Test with Sand Using DEM*. Archives of Hydro-Engineering and Environmental Mechanics, 56(3-4): 149-171.

WILLERT C.E., GHARIB M. 1991. *Digital particle image velocimetry*. Experiments in Fluids, 10(4): 181-193.

WU T.-R., HUANG C.-J., CHUANG M.-H., WANG C.-Y., C.-R. CHU C.-R. 2011. *Dynamic coupling of multi-phase fluids with a moving obstacle*. Journal of Marine Science and Technology, 19(6): 643-650.

XIANG J., LATHAM J.P., VIRE A., ANASTASAKI E, PAIN C.C. 2012. *Coupled fluidity/y3d technology and simulation tools for numerical breakwater modelling*. Coastal Engineering Proceedings, 33: 1-9.

ZENG Q., YAO J. 2015. *Numerical Simulation of Fluid-Solid Coupling in Fractured Porous Media with Discrete Fracture Model and Extended Finite Element Method*. Computation, 3: 541-557.

ZHAO J., SHAN T. 2013. *Coupled CFD–DEM simulation of fluid – particle interaction in geomechanics*, Powder Technology, 239: 248-258.